A 2,3′-Substituted Biphenyl-Based Amino Acid Facilitates the Formation of a Monomeric β-Hairpin-like Structure in Aqueous Solution at Elevated Temperature

Carey L. Nesloney and Jeffery W. Kelly*

Contribution from the Department of Chemistry, Texas A&M University, College Station, Texas 77843-3255

Received July 24, 1995[⊗]

Abstract: An evaluation of [3′-(2-aminoethyl)-2-biphenyl]propionic acid (**1**) and 2-amino-3′-biphenylcarboxylic acid (**2**) as β-sheet nucleators was accomplished by incorporating these residues into water soluble peptides. Residue **1** was designed to replace the backbone of the $i + 1$ and $i + 2$ residues of a β-turn and reverse the polypeptide chain direction via a hydrogen-bonded hydrophobic cluster to initiate β-hairpin folding. An NMR structural evaluation of heptapeptides incorporating **1** revealed the presence of a hydrophobic cluster involving an aromatic ring of **1** and a side chain of one of the flanking hydrophobic α-amino acids, even though the peptides lack sufficient length to adopt a β-sheet structure. The flanking α-amino acid residues in these peptides exhibit significantly slower amide proton/deuterium exchange rates, indicating that they are intramolecularly hydrogen bonded in aqueous solution. In appropriate tridecapeptides, the hydrogen-bonded hydrophobic cluster nucleates the formation of a β-hairpin structure which subsequently self-associates. Unlinking the intramolecular folding and self-association equilibria was accomplished by strategically replacing two of the exterior amide protons in the tridecapeptide with methyl groups. These tertiary amide groups cannot act as hydrogen bond donors and sterically block the intermolecular β-sheet interactions between exterior β-strands, preventing self-assembly. The N-methylated tridecapeptide incorporating **1** has been characterized by analytical equilibrium ultracentrifugation, far-UV CD, FT-IR, and a variety of NMR experiments which support a β-hairpin-like structure. Interestingly, these peptides exhibit an increase in β-sheet structure with increasing temperature which may prove to be general for β-sheets stabilized by hydrophobic interactions. The incorporation of residue **2** into an identical α-amino acid sequence does not result in folding under the same conditions, implying that the hydrogen-bonded hydrophobic cluster promoted by **1** is required for β-hairpin folding.

The mechanisms of β-sheet folding and the basis for sheet stability are under investigation in several laboratories using a variety of creative approaches.[1] While β-sheet structure is commonly observed in proteins, our understanding of this structural motif is poor relative to what is known about α-helical secondary structure. This is due, in part, to the difficulties inherent in creating a well-defined peptide model system for the detailed study of β-sheet formation in aqueous solution.[2] Although studies on the conformational propensities of peptides, amino acid homopolymers, and sequential copolymers has enhanced our understanding of β-sheet structure, the approach is limited because of competitive intra- and intermolecular folding which leads to heterogeneous aggregated β-sheet structures.[1q,3]

Biophysical studies regarding the folding mechanism(s) of β-sheet proteins suggest that the rate of refolding of a predominantly α-helical protein is roughly an order of magnitude faster than that of mostly β-sheet proteins, implying that the folding mechanisms may be quite different.[1a−d] Slow folding for β-sheets is consistent with the tertiary (nonlocal) nature of β-sheet structure.[4] The residue−residue interactions (hydro-

[⊗] Abstract published in *Advance ACS Abstracts,* June 1, 1996.

(1) (a) Finkelstein, A. V. *Proteins: Struct., Funct. Genet.* **1991**, *9*, 23−27. (b) Liu, Z.-P.; Rizo, J.; Gierasch, L. M. *Biochemistry* **1994**, *33*, 134−142. (c) Dyson, H. J.; Sayre, J. R.; Merutka, G.; Shin, H. C.; Lerner, R. A.; Wright, P. E. *J. Mol. Biol.* **1992**, *226*, 819−835. (d) Dyson, H. J.; Merutka, G.; Waltho, J. P.; Lerner, R. A.; Wright, P. E. *J. Mol. Biol.* **1992**, *226*, 795−817. (e) Kemp, D. S. *Trends Biotechnol.* **1990**, *8*, 249−255. (f) Minor, D. L., Jr.; Kim, P. S. *Nature* **1994**, *367*, 660−663. (g) Minor, D. L., Jr.; Kim, P. S. *Nature* **1994**, *371*, 264−267. (h) Smith, C. K.; Withka, J. M.; Regan, L. *Biochemistry* **1994**, *33*, 5510−5517. (i) Smith, C. K.; Regan, L. *Science* **1995**, *270*, 980−982. (j) Kim, C. A.; Berg, J. M. *Nature* **1993**, *362*, 267−270. (k) Erickson, B. W., Daniels, S. B., Higgins, M. L., Reddy, P. A. *Advances in Gene Technology: Protein Engineering and Production*; Oxford IRL Press: New York, 1988; pp 240. (l) Varley, P.; Gronenborn, A. M.; Christensen, H.; Wingfield, P. T.; Pain, R. H.; Clore, G. M. *Science* **1993**, *260*, 1110−1113. (m) Tsang, K. Y.; Díaz, H.; Graciani, N.; Kelly, J. W. *J. Am. Chem. Soc.* **1994**, *116*, 3988−4005. (n) Yan, Y.; Erickson, B. W. *Protein Sci.* **1994**, *3*, 1069−1073. (o) Blanco, F. J.; Rivas, G.; Serrano, L. *Struct. Biol.* **1994**, *1*, 584−590. (p) Fedorov, A. N.; Dolgikh, D. A.; Chemeris, V. V.; Chernov, B. K.; Finklestein, A. V.; Schulga, A. A.; Alakhov, Y. B.; Kirpichnikov, M. P.; Ptitsyn, O. B. *J. Mol. Biol.* **1992**, *225*, 927−931. (q) Zhang, S.; Holmes, T.; Lockshin, C.; Rich, A. *Proc. Natl. Acad. Sci. U.S.A.* **1993**, *90*, 3334−3338. (r) Hecht, M. H. *Proc. Natl. Acad. Sci. U.S.A.* **1994**, *91*, 8729−8730. (s) Quinn, T. P.; Tweedy, N. B.; Williams, R. W.; Richardson, J. S.; Richardson, D. C. *Proc. Natl. Acad. Sci. U.S.A.* **1994**, *91*, 8747−8751.

(2) (a) Creighton, T. E. *Proteins: Structure and Molecular Properties*, 2nd ed.; W. H. Freeman and Co.: New York, 1993. (b) Mattice, W. L. *Annu. Rev. Biophys. Biophys. Chem.* **1989**, *18*, 93−111. (c) Dyson, H. J.; Wright, P. E. *Annu. Rev. Biophys. Biophys. Chem.* **1991**, *20*, 519−538. (d) Yapa, K.; Weaver, D. L.; Karplus, M. *Proteins: Struct., Funct. Genet.* **1992**, *12*, 237−265.

(3) (a) Maeda, H.; Ooi, K. *Biopolymers* **1981**, *20*, 1549−1563. (b) Maeda, H.; Gatto, Y.; Ikeda, S. *Macromolecules* **1984**, *17*, 2031−2038. (c) Maeda, H. *Bull. Chem. Soc. Jpn.* **1987**, *60*, 3438−3440. (d) Brack, A.; Orgel, L. E. *Nature* **1975**, *256*, 383−387. (e) Brack, A.; Caille, A. *Int. J. Peptide Protein Res.* **1978**, *11*, 128−139. (f) Brack, A.; Spach, G. *J. Am. Chem. Soc.* **1981**, *103*, 6319−6323. (g) Johnson, B. J. *J. Pharm. Sci.* **1974**, *63*, 313−327. (h) Mattice, W. L.; Lee, E.; Scheraga, H. A. *Can. J. Chem.* **1985**, *63*, 140−146. (i) Rippon, W. B.; Chen, H. H.; Walton, A. G. *J. Mol. Biol.* **1973**, *75*, 369−375. (j) Seipke, G.; Arfmann, H. A.; Wagner, K. G. *Biopolymers* **1974**, *13*, 1621−1633. (k) Osterman, D. G.; Kaiser, E. T. *J. Cell. Biochem.* **1985**, *29*, 57−72. (l) DeGrado, W. F.; Lear, J. D. *J. Am. Chem. Soc.* **1985**, *107*, 7684−7689. (m) Rajasekharan Pillai, V. N.; Mütter, M. *Acc. Chem. Res.* **1981**, *14*, 122−130. (n) Choo, D. W.; Schneider, J. P.; Graciani, N. R.; Kelly, J. W. *Macromolecules* **1996**, *29*, 355−366. (o) Zhang, S.; Lockshin, C.; Cook, R.; Rich, A. *Biopolymers* **1994**, *34*, 663−672. (p) Krantz, D. D.; Zidovetzki, R.; Kagan, B. L.; Zipursky, S. L. *J. Biol. Chem.* **1991**, *266*, 16801−16807. (q) Ghadiri, M. R.; Granja, J. R.; Milligan, R. A.; McRee, D. E.; Khazanovich, N. *Nature* **1993**, *366*, 324−327. (r) Ghadiri, M. R.; Granja, J. R.; Buehler, L. K. *Nature* **1994**, *369*, 301−304. (s) Graciani, N. R.; Tsang, K. Y.; McCutchen, S. L.; Kelly, J. W. *Bioorg. Med. Chem.* **1994**, *2*, 999−1006. (t) Sun, X.; Lorenzi, G. P. *Helv. Chim. Acta* **1994**, *77*, 1520−1526.

S0002-7863(95)02472-3 CCC: $12.00

phobic and electrostatic) that facilitate strand−strand recognition and lead to a stable β-sheet motif in proteins generally involve residues that are far apart in sequence, unlike the situation in an α-helical secondary structure where localized i and $i + 4$ residue interactions facilitate rapid folding. An evaluation of the thermodynamic β-sheet propensities of the α-amino acids reveals a definite context dependence, implying that the contribution of a given residue to the stability of a β-sheet depends on both local and nonlocal residue−residue interactions.[1f−j] It follows that the more complex the topology of a given β-sheet, the more tertiary-like the structure is, making the design of such a sheet quite complicated.

One goal of the study presented within is to develop a reliable strategy to prepare monomeric β-hairpin structures that can accommodate considerable α-amino acid sequence variation. In principle, this could also be accomplished using a consensus β-turn sequence. However, the conformational propensities of known β-turn sequences do not appear to be sufficient to effect β-hairpin folding, given what is currently known about the process.[1c,5] Therefore, unnatural amino acid templates designed to initiate β-sheet folding are being developed by several laboratories, taking advantage of the template concept first reported by Hirschmann and co-workers in their work on cyclic somatostatin analogues.[1m,3ns,6] Here we outline the utility of template **1** (Figure 1a) which was designed to replace the backbone of the $i + 1$ and $i + 2$ residues of a β-turn and reverse the polypeptide chain direction via a hydrogen-bonded hydrophobic cluster conformation to initiate β-hairpin folding.

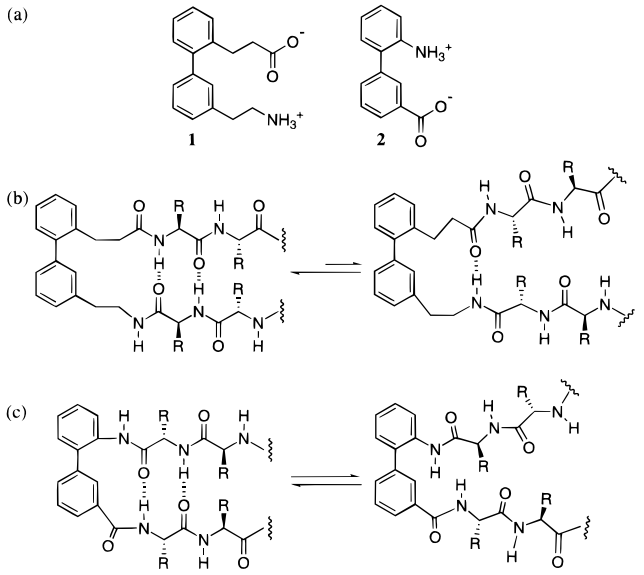

Figure 1. (a) Structures of biphenyl-based amino acids 3′-(2-aminoethyl)-2-biphenylpropionic acid (**1**) and 2-amino-3′-biphenylcarboxylic acid (**2**). (b) For peptides containing **1**, both the 13- and 15-membered hydrogen-bonded ring conformations are possible, with the 15-membered ring being favored. (c) For peptides containing **2**, the 11-membered hydrogen-bonded ring conformation is favored.

The previously reported solid and solution state (FT-IR and variable temperature ^{1}H NMR) structures of a diamide derivative of **1** in CH_2Cl_2 suggest that peptides composed of residue **1** will most likely adopt a conformation where the α-amino acid residues flanking **1** are intramolecularly hydrogen bonded, leaving the carbonyl and NH derived from **1** to hydrogen bond with water (Figure 1b).[7] The $-CH_2CH_2-$ linker connecting the biphenyl substructure to the peptides in **1** prefers to adopt a low energy perpendicular conformation where the aliphatic carbon-carbon bond in the phenethyl fragment is oriented perpendicular to the plane of the aromatic ring.[7,8] Molecular dynamics/mechanics studies on peptides incorporating **1** indicate that this conformational preference makes it feasible for one of the hydrophobic side chains of the flanking α-amino acids to interact with the biphenyl substructure of **1** while maintaining idealized intramolecular hydrogen bonding between the flanking α-amino acids, leading to a hydrogen-bonded hydrophobic cluster (Figure 2). Hydrophobic clusters are evolving as important intermediates in the folding of both peptides and proteins and appear to reduce the local entropy penalty for folding by preorganizing the "unfolded state".[1m,9] The FT-IR and ^{1}H NMR studies on a diamide derivative of **2** in CH_2Cl_2 suggest that intramolecular hydrogen bonding between the flanking amino acids in peptides containing **2** (Figure 1c) will not be appreciably stabilized relative to the non-hydrogen-bonded state in aqueous solution.[7] The absence of the $-CH_2-CH_2-$ linker in residue **2** significantly restricts the flexibility of the attached strands, interfering with the ability of the molecule to form a hydrophobic cluster. Therefore, the expectation is that residue **1** will be able to nucleate sheet

(4) (a) Lifson, S.; Sander, C. *J. Mol. Biol.* **1980**, *139*, 627−639. (b) Nesloney, C. L.; Kelly, J. W. *Bioorg. Med. Chem.*, in press. (c) Schneider, J. P.; Kelly, J. W. *Chem. Rev.* **1995**, *95*, 2169−2187.

(5) Several small peptides are capable of populating a β-turn conformation; see: (a) Rose, G. D.; Gierasch, L. M.; Smith, J. A. *Adv. Protein Chem.* **1985**, *17*, 1−109. (b) Rizo, J.; Gierasch, L. M. *Annu. Rev. Biochem.* **1992**, *61*, 387−418. (c) Dyson, H. J.; Cross, K. J.; Houghten, R. A.; Wilson, I. A.; Wright, P. E.; Lerner, R. A. *Nature* **1985**, *318*, 480. (d) Hruby, V. J. In *Chemistry and Biochemistry of Amino Acids*; Weinstein, B., Ed.; M. Dekker: New York, 1974; Vol. 3, pp 1−188. (e) Hruby, V. J.; Al-Obeidi, F.; Kazmierski, W. *Biochem. J.* **1990**, *268*, 249−262. (f) Hruby, V. J. *Life Sci.* **1982**, *31*, 189−199. However, concensus β-turn sequences do not appear to be sufficient to nucleate folding within sequences which are known to fold when nucleated by unnatural amino acids such as the 4-(2-aminoethyl)-6-dibenzofuranpropionic acid, unpublished results.

(6) (a) Díaz, H.; Kelly, J. W. *Tetrahedron Lett.* **1991**, *32*, 5725−5728. (b) Díaz, H.; Espina, J. R.; Kelly, J. W. *J. Am. Chem. Soc.* **1992**, *114*, 8316−8318. (c) Díaz, H.; Tsang, K. Y.; Choo, D.; Espina, J. R.; Kelly, J. W. *J. Am. Chem. Soc.* **1993**, *115*, 3790−3791. (d) Díaz, H.; Tsang, K. Y.; Choo, D.; Kelly, J. W. *Tetrahedron* **1993**, *49*, 3533−3545. (e) Schneider, J. P.; Kelly, J. W. *J. Am. Chem. Soc.* **1995**, *117*, 2533−2546. (f) Kemp, D. S.; Bowen, B. R. *Tetrahedron Lett.* **1988**, *29*, 5081−5082. (g) Kemp, D. S.; Bowen, B. R. *Tetrahedron Lett.* **1988**, *29*, 5077−5080. (h) Kemp, D. S.; Bowen, B. R.; Muendel, C. C. *J. Org. Chem.* **1990**, *55*, 4650−4657. (i) Mütter, M. *Trends Biochem. Sci.* **1988**, *13*, 260. (j) Mütter, M.; Vuilleumier, S. *Angew. Chem., Int. Ed. Engl.* **1989**, *28*, 535. (k) Brandmeier, V.; Feigel, M. *Tetrahedron* **1989**, *45*, 1365−1376. (l) Brandmeier, V.; Feigel, M.; Bremer, M. *Angew. Chem., Int. Ed. Engl.* **1989**, *28*, 486−488. (m) Brandmeier, V.; Sauer, W. H. B.; Fiegel, M. *Helv. Chim. Acta* **1994**, *77*, 70−85. (n) Wagner, G.; Feigel, M. *Tetrahedron* **1993**, *49*, 10831−10842. (o) Feigel, M. *J. Am. Chem. Soc.* **1986**, *108*, 181−182. (p) Sato, K.; Nagai, U. *J. Chem. Soc., Perkin Trans. 1* **1986**, 1231−1234. (q) Gardner, R. R.; Liang, G.-B.; Gellman, S. H. *J. Am. Chem. Soc.* **1995**, *117*, 3280−3281. (r) Nowick, J. S.; Powell, N. A.; Martinez, E. J.; Smith, E. M.; Noronha, G. *J. Org. Chem.* **1992**, *57*, 3763−3765. (s) Nowick, J. S.; Smith, E. M.; Noronha, G. *J. Org. Chem.* **1995**, *60*, 7386−7387. (t) Veber, D. F.; Strachan, R. G.; Bergstrand, S. J.; Holly, F. W.; Homnick, C. F.; Hirschmann, R. J. *J. Am. Chem. Soc.* **1976**, *98*, 2367−2369. (u) Veber, D. F.; Holly, F. W.; Paleveda, W. J.; Nutt, R. F.; Bergstrand, S. J.; Torchiana, M.; Glitzer, M. S.; Saperstein, R.; Hirschmann, R. *Proc. Natl. Acad. Sci. U.S.A.* **1978**, *75*, 2636−2640. (v) Veber, D. F.; Saperstein, R.; Nutt, R. F.; Freidinger, R. M.; Brady, S. F.; Curley, P.; Perlow, D. S.; Palveda, W. J.; Colton, C. D.; Zacchei, A. G.; Toco, D. J.; Hoff, D. R.; Vandlen, R. L.; Gerich, J. E.; Hall, L.; Mandarino, L.; Cordes, E. H.; Anderson, P. S.; Hirschmann, R. *Life Sci.* **1984**, *34*, 1371−1378. (w) Freidinger, R. M.; Veber, D. F.; Schwenk Perlow, D. *Science* **1980**, *210*, 656−658.

(7) Nesloney, C. L.; Kelly, J. W. *J. Org. Chem.* **1996**, *61*, 3227−3237.

(8) (a) Scharfenberg, P.; Rozsondai, B.; Hargittai, I. *Z. Naturforsch., A* **1980**, *35a*, 431−436. (b) Kriz, J.; Jakes, J. *J. Mol. Struct.* **1972**, *12*, 367−372.

(9) (a) Dill, K. A. *Biochemistry* **1990**, *29*, 7133−7155. (b) Kauzmann, W. *Adv. Protein Chem.* **1959**, *14*, 1−63. (c) Rose, G. D.; Roy, S. *Proc. Natl. Acad. Sci. U.S.A.* **1980**, *77*, 4643. (d) Neri, D.; Billeter, M.; Wider, G.; Wüthrich, K. *Science* **1992**, *257*, 1559−1563. (e) Topping, K. D.; Evans, P. A.; Dobson, C. M. *Proteins: Struct., Funct. Genet.* **1991**, *9*, 246. (f) Garvey, E. P.; Swank, J.; Matthews, C. R. *Proteins: Struct., Funct. Genet.* **1989**, *6*, 259−266.

Table 1. Primary Sequences of Peptides **A**−**H**

peptide[a]	R1	R2	R3	R4	R5	R6	R7	R8	R9	R10	R11	R12	R13
A				Val	Orn	Leu	**1**	Val	Orn	Leu			
B				Val	Orn	Phe	**1**	Val	Orn	Leu			
C				Val	Glu	Leu	**1**	Val	Orn	Leu			
D	Lys	Val	Lys	Val	Lys	Leu	**1**	Val	Lys	Val	Lys	Val	Lys
E	Lys	Val	Lys	Val	Lys	Leu	**2**	Val	Lys	Val	Lys	Val	Lys
F	Val	Lys	Val	Lys	Val	Lys	**1**	Lys	Val	Lys	Val	Lys	Val
G	Lys	Val	*N*-Me-Leu	Val	Lys	Leu	**1**	Val	Lys	Val	*N*-Me-Leu	Val	Lys
H	Lys	Val	Lys	Val	Lys	Val	**GG**	Val	Lys	Val	Lys	Val	Lys

[a] Sequences are written from the N-terminus to the C-terminus which in all cases is a primary amide ($C(O)NH_2$).

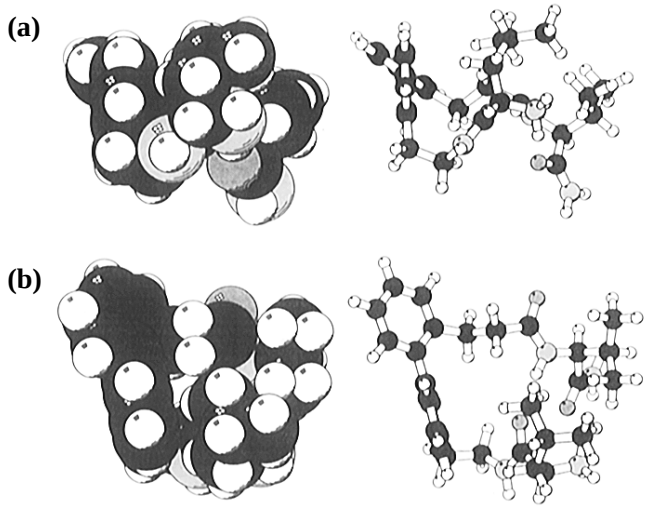

Figure 2. Molecular Graphics representation[28] of -Leu-**1**-Val- demonstrating the hydrophobic cluster conformation in which the ethyl side chains of **1** are perpendicular to the aromatic rings and hydrophobic interactions between one ring and the leucine side chain are present. The structure represents the lowest energy conformation predicted by molecular mechanics/molecular dynamics of the peptide H_3N-VOL-**1**-VOL-$C(O)NH_2$ in aqueous solution: (a) side view; (b) top view.

formation by facilitating the formation of a hydrogen-bonded hydrophobic cluster, whereas residue **2** will not.

Generally, the α-amino acid sequences in this study were chosen by considering the β-sheet forming propensity of each residue, the long-range residue−residue interactions which hold the hairpin together, the amphiphilicity of the sequence, and the overall charge of each peptide to ensure solubility.[1f−j,10] Sequences incorporating templates **1** and **2** were usually designed such that the strand-reversing residues are flanked by hydrophobic α-amino acids to facilitate hydrophobic cluster formation (Table 1).

We and others have found that successful β-hairpin designs self-associate into cross-β-structures, as a result of the thermodynamic stability of this quaternary structure.[3n,11] This unwanted self-assembly of an intramolecularly folded β-sheet (hairpin) structure has proven to be a common problem in attempts to prepare monomeric or well-defined β-sheet model systems.[1q,3d−e,n−o,12] The same side chain−side chain interactions and hydrogen bonds that facilitate intramolecular β-sheet folding also favor intermolecular β-sheet-mediated self-assembly. One strategy to avoid β-hairpin-mediated self-association is to eliminate the potential for hydrogen bonding and to sterically prevent the strand−strand interactions required for intermolecular β-sheet formation by replacing the exterior amide protons with methyl groups. The resulting tertiary amide bonds strongly prefer the *trans* conformation required for β-sheet formation.[13] The concept of replacing an amide proton with a methyl group in order to prevent lateral β-sheet-mediated self-association has been successfully demonstrated in preventing the dimerization of interleukin-8 (IL-8) and in preventing the self-assembly of nanotubes formed via intermolecular sheet formation.[3t,14] Solid state or NMR structures on IL-8, a nanotube dimer, and an N-methylated derivative of Gramicidin S indicate that the incorporation of an N-methylated amino acid into an α-amino acid sequence which favors β-sheet formation does not significantly perturb the resulting β-sheet structure.[14b,15]

Residues **1** and **2** were incorporated into several α-amino acid sequences, some containing N-methylated α-amino acids, to compare their ability to nucleate β-sheet formation and to understand their mechanism of function where appropriate. Here, we present evidence that a new biphenyl-based amino acid template (**1**) promotes β-hairpin folding, affording either monomeric or self-assembled β-sheet structures.

Results

Synthesis of Peptides A−G. Details regarding the preparation of the 2,3′-substituted biphenyl-based amino acids **1** and **2** are published elsewhere.[7] Peptides **A**−**G** were synthesized on benzhydrylamine resin employing standard *t*-Boc synthesis procedures (with BOP activation) to incorporate the α-amino acids and the *t*-Boc derivative of **1** into the growing peptide chain.[1m] Due to the poor reactivity of the aniline functionality of **2**, residue **2** was incorporated into peptides as a dipeptide (*t*-Boc-Leu-**2**-CO_2H) prepared in solution and coupled to the resin bound peptide by BOP activation. The peptides were deprotected and cleaved from the resin using high-HF[16] and purified by reversed phase C_{18} HPLC. The primary structures

(10) Kaiser, E. T.; Kézdy, F. J. *Science* **1984**, *223*, 249−255.
(11) (a) Kelly, J. W.; Lansbury, P. T., Jr. *Amyloid: Int. J. Exp. Clin. Invest.* **1994**, *1*, 186−205. (b) Lansbury, P. T., Jr. *Biochemistry* **1992**, *31*, 6865.
(12) Hartman, R.; Schwaner, R. C.; Hermans, J. *J. Mol. Biol.* **1974**, *90*, 415−429.
(13) (a) Tonelli, A. E. *J. Am. Chem. Soc.* **1970**, *92*, 6187−6190. (b) Tonelli, A. E. *J. Am. Chem. Soc.* **1971**, *93*, 7153−7155. (c) Tonelli, A. E. *J. Mol. Biol.* **1974**, *86*, 627−635. (d) Tonelli, A. E. *Biopolymers* **1976**, *15*, 1615−1622. (e) Tonelli, A. E.; Patel, D. J. *Biopolymers* **1976**, *15*, 1623. (f) Vitoux, B.; Aubry, A.; Cung, M. T.; Marraud, M. *Int. J. Peptide Protein Res.* **1986**, *27*, 617−632.
(14) (a) Rajarathnam, K.; Sykes, B. D.; Kay, C. M.; Dewald, B.; Geiser, T.; Baggiolini, M.; Clark-Lewis, I. *Science* **1994**, *264*, 90−92. (b) Ghadiri, M. R.; Kobayashi, K.; Granja, J. R.; Chadha, R. K.; McRee, D. E. *Angew. Chem., Int. Ed. Engl.* **1995**, *34*, 93−95.
(15) (a) Kumar, N. G.; Izumiya, N.; Miyoshi, M.; Sugano, H.; Urry, D. W. *Biochemistry* **1975**, *14*, 2197−2207. (b) Patel, D. J.; Tonelli, A. E. *Biopolymers* **1976**, *15*, 1623−1635.
(16) Tam, J. P.; Merrifield, R. B. In *The Peptides; Analysis, Synthesis, and Biology*; Udenfriend, S., Meienhofer, J., Eds.; Academic Press: New York, 1987; pp 185−244.

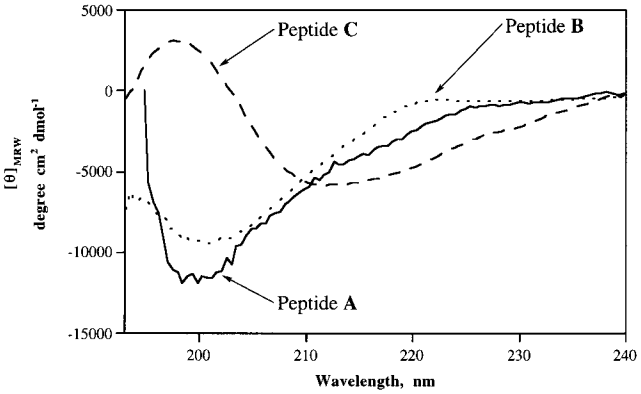

Figure 3. Circular dichroism spectra of 0.17 mM peptide **A**, pH 6.8; 0.26 mM peptide **B**, pH 7.2; and 0.26 mM peptide **C**, pH 6.8. Spectra were obtained at 25 °C in 10 mM Tris buffer. Spectra were corrected for buffer contributions and are reported in units of mean residue ellipticity.

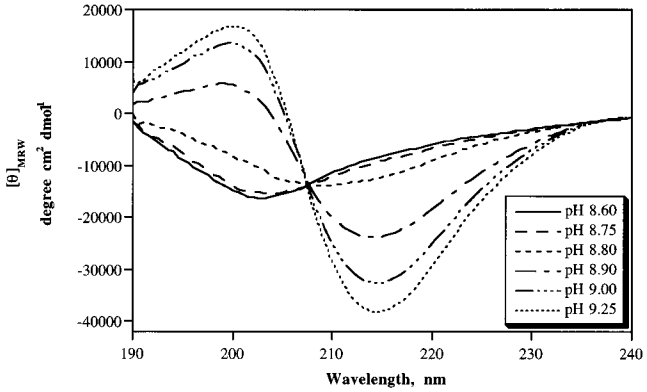

Figure 4. Circular dichroism study of the pH dependence of 0.15 mM peptide **D**. Spectra were obtained at 25 °C in 10 mM borate buffer. Spectra were corrected for buffer contributions and are reported in units of mean residue ellipticity.

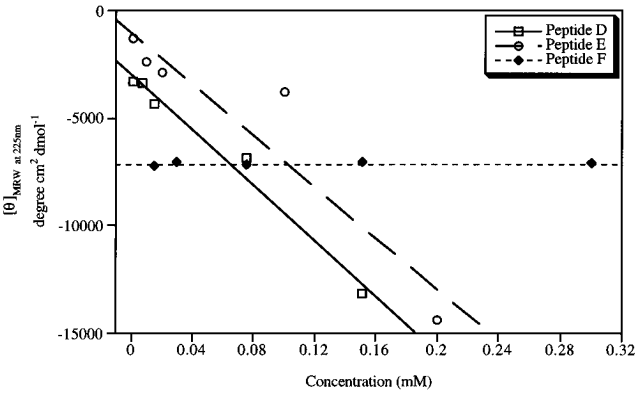

Figure 5. Concentration dependence of peptide **D** (pH 9.1, 214 nm), peptide **E** (pH 10.6, 215 nm), and peptide **G** (pH 7.0, 224 nm). Concentration versus the mean residue ellipticity is plotted.

of peptides **A**−**G** were confirmed by nominal resolution matrix-assisted laser desorption mass spectrometry.[17]

Circular Dichroism Studies of Peptides A−F. Residue **1** was incorporated into three heptapeptide sequences based on the cyclic peptide Gramicidin S. One of the two D-Phe-Pro dipeptide units (the $i + 1$ and $i + 2$ dipeptides of the two β-turns) of Gramicidin S was replaced by residue **1** while the other was omitted from the sequence, affording an acyclic peptide. Heptapeptide **A** has an α-amino acid sequence homologous to a 4-(2-aminoethyl)-6-dibenzofuranpropionic acid-based heptapeptide studied previously by our laboratory,[1m,6c,d] allowing us to compare the efficacy of the biphenyl- and dibenzofuran-based amino acids as nucleators in a homologous α-amino acid sequence. Peptide **B**, having a Phe in place of Leu-3, was prepared to test the feasibility of using an aromatic−aromatic interaction to stabilize the hydrophobic cluster and facilitate β-sheet folding.[18] In peptide **C**, ornithine-2 was replaced with Glu to probe the effect of an additional long-range residue−residue electrostatic interaction (salt bridge) on β-sheet stability in the context of a heptapeptide. Evaluation of peptides **A** and **B** by far-UV circular dichroism (CD) reveals that these peptides exist as a random coil in aqueous solution over a pH range of 4−9. The CD spectra exhibit minima at 200 nm, consistent with a rapidly interconverting ensemble of conformations (Figure 3). The analogous 4-(2-aminoethyl)-6-dibenzofuranpropionic acid-based heptapeptides exhibit fluctuating β-sheet structures under these conditions.[1m] Peptide **C** adopts a random coil structure at pH 5 (minimum 201 nm). However, at pH 7, a coil to soluble associated β-sheet transition is observed as discerned from a CD maximum at 193 nm and a minimum at 214 nm (Figure 3). Most likely deprotonation of Glu-2 allows the formation of both intramolecular and intermolecular salt bridges which contribute to the added stability of this β-sheet quaternary structure (*vide infra*). As expected, the intramolecular folding and the self-association equilibria are linked as discerned from the observation of an insoluble β-sheet structure at pH values > 7.5 (peptide concentration of 0.25 mM).

The tridecameric peptides **D**−**F** (Table 1) were studied by far-UV CD to determine whether the incorporation of **1** and **2** into longer amphiphilic peptides would result in β-sheet folding. These sequences are similar to the repeating $(Val\text{-}Lys)_n$ sequential polypeptides ($n > 25$) which are known to undergo a coil to self-associated β-sheet transition at pH 8.9.[3d,n,12] The high charge density on peptides **D** and **E** should prevent the favorable strand−strand interactions required for sheet formation at low pH. The removal of two or more of the charges on the Lys ϵ-ammonium groups effected by increasing the pH is expected to facilitate intramolecular folding followed by self-assembly.[3n] A leucine was employed as one of the flanking residues in these peptides instead of valine because the increased side chain flexibility should maximize packing interactions required for hydrophobic cluster formation. Interestingly, peptide **D** undergoes a marked transition from a random coil (minimum at 203 nm) to a β-sheet (maximum at 201 nm, minimum at 214 nm) from pH 8.6 to pH 9.0 (Figure 4). The folding transition from a random coil to a β-sheet exhibited by peptide **D** appears to be a simple two-state transition, as implied by the isodichroic point at 207 nm in the pH dependent far-UV CD spectra. However, the linear concentration dependence of the far-UV CD spectra of peptide **D** suggests that it is undergoing self-association subsequent to intramolecular folding (Figure 5). Peptide **D** exists as a mixture of random coil and β-sheet structures at concentrations below 0.075 mM and as a self-associated β-sheet over the concentration range of 0.075−0.15 mM (pH 9.3). These results and those for peptide **C** imply that self-assembly significantly stabilizes the metastable intramolecularly folded β-sheet state (*vide infra*), implying that **1** is capable of nucleating intramolecular β-sheet folding in appropriate sequences. Peptide **E** is identical to peptide **D** except that it incorporates residue **2** in place of residue **1**. Peptide **E** exists as a random coil (minimum at 204 nm) over a pH range of 4−9.8 at a peptide concentration of 0.20 mM

(17) (a) Chait, B. T.; Kent, S. B. H. *Science* **1992**, *257*, 1885. (b) Kinsel, G. R.; Preston, L. M.; Russell, D. H. *Biol. Mass Spectrom.* **1994**, *23*, 205−211.

(18) Paliwal, S.; Geib, S.; Wilcox, C. S. *J. Am. Chem. Soc.* **1994**, *116*, 4497−4498.

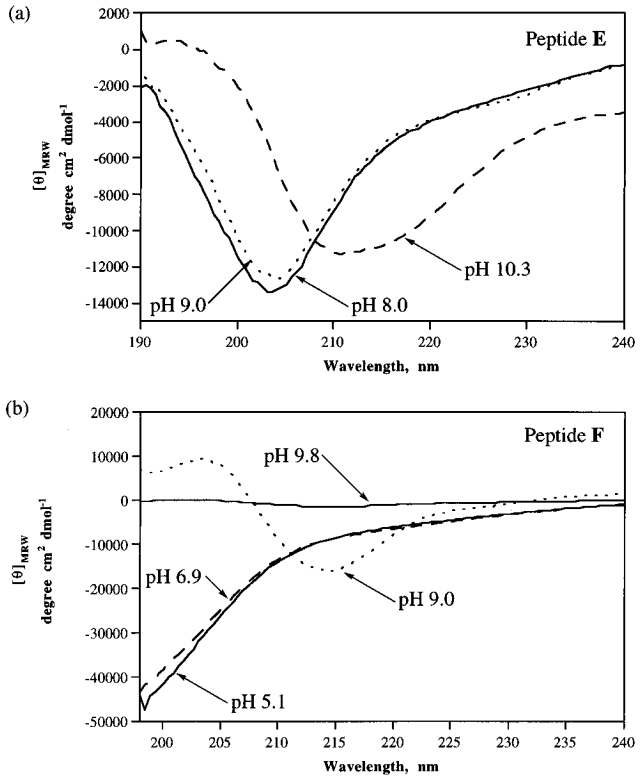

Figure 6. Circular dichroism study of the pH dependence of (a) 0.20 mM peptide **E** and (b) 0.25 mM peptide **F**. Spectra were obtained at 25 °C in 10 mM acetate buffer (pH 5.1), 10 mM Tris buffer (pH 6.9), and 10 mM borate buffer (pH 8.0−10.3). Spectra were corrected for buffer contributions and are reported in units of mean residue ellipticity.

(Figure 6a), suggesting that **2** is not capable of forming the hydrogen-bonded hydrophobic cluster necessary for initiating β-sheet structure under conditions where peptide **D** adopts a β-sheet structure. A β-sheet structure is observed in peptide **E** at pH values > 10. However, the lack of an isodichroic point suggests that the coil to aggregated sheet structure is not well defined; i.e., intramolecular folding does not precede self-assembly.[19] The concentration dependence of the CD spectra of peptide **E** (Figure 5) suggests a self-associating β-sheet at concentrations above 0.20 mM at pH 10.6. Peptide **F** was prepared to probe the importance of hydrophobic cluster formation in β-sheet folding mediated by residue **1**. The flanking hydrophobic residues in peptide **D** were replaced with hydrophilic lysine residues in peptide **F** while maintaining a highly homologous amino acid composition and an amphiphilic periodicity of 2. A 0.25 mM solution of peptide **F** is incapable of folding at pH 8.9, whereas 0.15 mM samples of peptide **D** adopt a β-sheet structure at this pH, implying that hydrophobic cluster interactions are critical for the function of **1**. Peptide **F** will adopt a β-sheet structure above pH 9 (Figure 6b), which may be explained by deprotonation of one of the two ϵ-ammonium groups of the flanking Lys residues, allowing packing against one of the phenyl rings in **1**. More likely, intermolecular sheet formation is occurring as observed in (Val-Lys)$_n$ sequences. A self-association mechanism is supported by precipitation of insoluble aggregates above pH 9.8.

^{1}H NMR Studies of Peptides A and D−F. Classical NOESY and TOCSY experiments have been utilized to make sequence-specific resonance assignments for peptide **A**. The flanking residues of peptides **D**−**F** were similarly assigned. The remaining valine and lysine spin systems in peptides **D**−**F** were identified but not sequence specifically assigned due to resonance overlap.

Strong NOEs between the aromatic protons of residue **1** and the flanking Leu-3 δ- and δ'-methyl groups and the Val-5 γ- and γ'-methyl groups of peptide **A** were observed. NOEs were also evident between the aromatic protons of **1** and the γ-methylene proton of Leu-3 in this peptide. Peptide **D** exhibits analogous NOEs between the aromatic protons of residue **1** and the methyl groups of the flanking Val and Leu residues. Additional NOEs were seen between the aromatic protons and the Leu-6 β-, β'-, and γ-protons in peptide **D**. The observed NOEs support the existence of a hydrophobic cluster composed of the aromatic skeleton of residue **1** and the hydrophobic residues flanking **1** in both peptides **A** and **D**.[9d] Importantly, the NMR data were collected under conditions where these peptides are "unstructured" by far-UV CD. Hence, the hydrophobic cluster appears to be structurally organized and poised to nucleate β-sheet formation once solution conditions permit strand−strand interactions. This is consistent with other studies on peptides and proteins where hydrophobic clusters are observed to be stable under "denaturing" conditions and in the absence of a regular protein structure as discerned by far-UV CD.[9] NOEs between the aromatic protons of residue **1** and the methylene groups of the flanking hydrophilic lysine side chains were not observed in peptide **F**. The inability of the lysine side chains to facilitate the formation of a hydrophobic cluster at pH values below the pK_a of the ϵ-ammonium group (pH > 8.9) has also been observed in 4-(2-aminoethyl)-6-dibenzofuranpropionic acid-based heptapeptides, implying that alkyl side chains with an ammonium group at the terminus cannot pack efficiently against an aromatic ring.[1m] The methylene protons in the lysine side chains of peptide **F** exhibit no discernible upfield shift consistent with the lack of cluster formation at pH values < 8.9.

The lack of observed NOEs between the aromatic protons of residue **2** and the methyl groups of the flanking valine and leucine residues in peptide **E** suggest that residue **2** cannot promote hydrophobic cluster formation consistent with the decreased flexibility of this residue. The methyl groups of the flanking Leu and Val residues in peptides **A**, **D**, and **E** exhibit upfield shifts of 0.1−0.2 ppm relative to those of the other valine residues in these sequences. The upfield shifts suggest that these peptides sample conformations where the methyl groups are in the diamagnetic shielding cones of the biphenyl ring systems of **1** and **2**. However, the observation of an upfield shift alone is not an indication of hydrophobic cluster formation since **2** cannot promote hydrophobic cluster formation.[20]

Information concerning the hydrogen-bonding network within a peptide containing residue **1** in aqueous solution was obtained from amide exchange studies of peptide **A** (3.0−3.3 mM, pH 3.4−3.6) and peptide **D** (2.5−2.9 mM, pH 4.1−5.1) where peptides **A** and **D** appear to be unstructured by far-UV CD. In both peptides, the rates of amide proton/deuterium exchange for the Leu and Val residues flanking **1** were at least an order of magnitude slower than the measurable rates for the remaining residues (Table 2). This suggests that the amide protons of the α-amino acid residues flanking **1** are being protected from amide

(19) The higher concentration of peptide **E** (0.20 mM) versus peptide **D** (0.15 mM) in these studies increases the likelihood of stabilizing an intramolecular sheet by self-assembly. However, no structure is observed over the pH range of 4−9.8, providing strong evidence that peptide **E** does not form intramolecular β-sheet structure under these conditions.

(20) An additional conformation for peptides **A** and **E** is suggested by their 1-D NMR spectra. A small triplet corresponding to the δ'-CH_3 group of Leu-3 in peptide **A** and Leu-6 in peptide **E** was also observed. The significant increase in upfield shifting (0.3 ppm relative to that of the remaining valine methyl groups) suggests the presence of a closer interaction between the leucine δ'-methyl group and one of the aromatic rings of the biphenyl system.

Table 2. Amide Proton Exchange Rates for Peptides **A** and **D**[a]

peptide **A** NHs	k_{ex} (min^{-1})	peptide **D** NHs	k_{ex} (min^{-1})
Orn-6	0.21	Val	0.25
Orn-2, Leu-7	0.18	Val, Lys	0.31
Leu-3[b]	0.019	Val, Leu-6[b]	0.041
Val-5[b]	0.034	Val-8[b]	0.042
$ArCH_2CH_2NH$		$ArCH_2CH_2NH$	
Val-1		Val, 5 Lys	

[a] Peptide **A** was 3.0−3.3 mM at pH 3.4−3.6. Peptide **D** was 2.2−2.4 mM at pH 4.1−5.1. The rates were determined at 25 °C for at least three experiments, and the averaged values are reported. [b] Amino acids which flank residue **1**.

exchange by intramolecular hydrogen bonding. The residue specific amide NH assignments in combination with the amide exchange data strongly suggest that residue **1** promotes a 15-membered hydrogen-bonded ring conformation in aqueous solution; i.e., the α-amino acid residues flanking **1** hydrogen bond with each other. In both peptides **A** and **D**, the amide proton of residue **1** exchanged too quickly to be observed within the time required to obtain the first NMR spectrum, suggesting that this amide proton is solvent exposed.

On the basis of the NMR and CD data, it appears that peptides incorporating the subsequence −hydrophobic α-amino acid−**1**−hydrophobic α-amino acid− adopt a hydrogen-bonded hydrophobic cluster conformation which can nucleate antiparallel β-sheet structure provided that the remaining α-amino acid sequence is appropriate to support a β-sheet structure. Conversely, peptides incorporating residue **2** are incapable of forming an intramolecular β-sheet structure presumably due to the inability of residue **2** to form a hydrogen-bonded hydrophobic cluster.

Determination of the Quaternary Structure of Peptide D. An associated, but soluble, β-sheet structure appears to form for peptides **C** and **D** as discerned from the pH and concentration dependent far-UV CD spectra. Insoluble aggregates were also observed for peptide **C** at higher concentrations (e.g., 0.25 mM) and/or pH values > 7.5. Insoluble aggregates were observed for peptide **D** under highly alkaline conditions (pH > 10, 0.15 mM). The implication behind these observations is that the intramolecular folding and self-association equilibria are linked. The solution molecular weight of peptide **D** was evaluated by analytical equilibrium ultracentrifugation under conditions where β-sheet structure is observed by far-UV CD (e.g., 0.15 mmol, pH 9.1). The sedimentation of peptide **D** to the bottom of the ultracentrifugation cell was observed even at low rotor speeds, indicating that this peptide adopts a highly associated soluble β-sheet structure.

The soluble high molecular weight assemblies of peptide **D** were absorbed onto a carbon-coated copper grid from a 0.041 mM solution at pH 10.2 (10 mM borate buffer) and visualized with Ruthenium Red stain[21] at a magnification of 80000× by electron microscopy. The observed fibrils typically had dimensions of ∼30 Å by 500−1000 Å. These dimensions are consistent with a cross-β-like structure in which the peptide has undergone intramolecular folding followed by self-assembly via intermolecular β-sheet formation. Fibril−fibril assemblies with widths of greater that 50 Å were also observed presumably as a result of protofilament assembly. It appears from these studies that peptide **D** undergoes intramolecular folding followed by self-association to afford a cross-β-sheet structure.

Characterization of Peptide G. The CD studies of peptide **D** suggest that the biphenyl-based amino acid **1** nucleates intramolecular antiparallel β-sheet folding, leading to a preorganized monomeric β-sheet structure which spontaneously self-associates into a high molecular weight, cross-β-sheet structure. It seems reasonable that the incorporation of N-methylated amino acid residues into peptide **D** would unlink the folding and assembly equilibria, allowing a monomeric or dimeric β-sheet to be observed. Hence, peptide **G** (Table 1) was prepared to demonstrate that peptide **D** adopts a β-hairpin conformation prior to self-assembly. The sequence of peptide **G** is identical to that of peptide **D** except that the Lys-3 and Lys-11 residues have been replaced with N-methylated Leu residues. The far-UV CD spectra of peptide **G** at 25 °C exhibit little dependence on pH (Figure 7a), demonstrating that the replacement of two of the six Lys residues with noncharged residues affords a sheet structure which folds in a pH independent manner.[3n] The CD spectra exhibit minima at 198 and 223 nm, indicating that peptide **G** adopts both random coil and β-sheet structure (Figure 7a). This observation is consistent with the peptide being structured in the region close to the β-turn and less structured at the termini of the strands due to fraying (*vide infra*). Also of interest is the shift of the β-sheet minimum to longer wavelengths relative to that of peptide **D** (223 nm versus 214 nm). Upon heating, peptide **G** exhibits an increase in β-sheet structure with a corresponding decrease in the random coil CD signal, but does not aggregate (Figure 7b). This temperature sensitive increase in β-sheet structure is in accord with the anticipated importance of the hydrophobic effect toward the stability of the β-sheet structure in peptide **G**.[22] The concentration dependent far-UV CD study of peptide **G** indicates that the peptide is monomeric as the mean residue ellipticity (225 nm) remains constant over a concentration range of 0.015−0.4 mM (pH 7) (Figure 5). Additionally, this peptide is monomeric within the concentration and pH ranges studied as

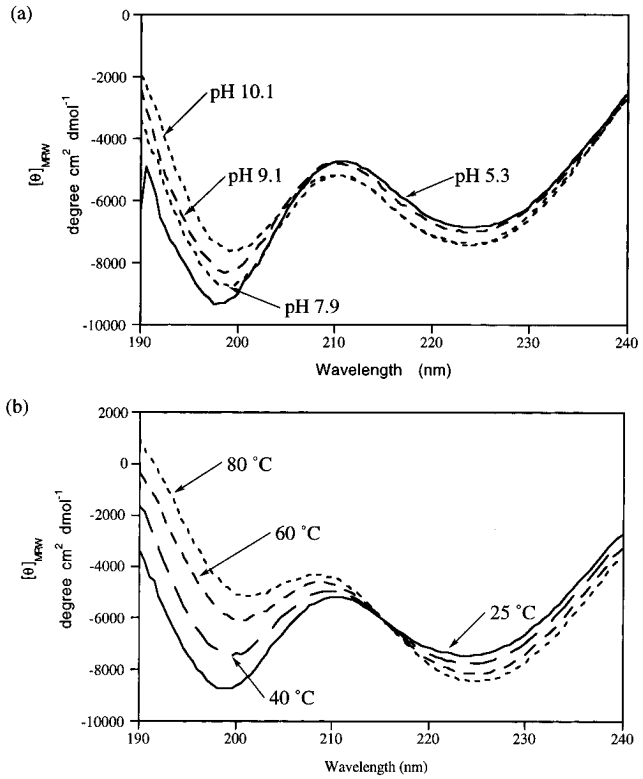

Figure 7. Circular dichroism study of the (a) pH dependence at 25 °C and (b) temperature dependence at pH 7.9 of 0.15 mM peptide **G**. Spectra were obtained in 10 mM acetate buffer (pH 4.1−5.3) and 10 mM borate buffer (pH 7.9−10.1). Spectra were corrected for buffer contributions and are reported in units of mean residue ellipticity.

(21) Kobayasi, T.; Asboe-Hansen, G. *J. Microsc.* **1971**, *93*, 55−60.

(22) Urry, D. W.; Luan, C.-H.; Parker, T. M.; Gowda, D. C.; Prasad, K. U.; Reid, M. C.; Safavy, A. *J. Am. Chem. Soc.* **1991**, *113*, 4346−4348.

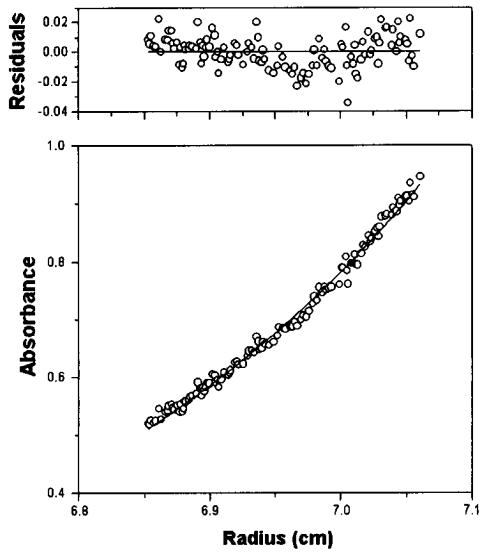

Figure 8. First pass analysis of the equilibrium ultracentrifugation data (60 000 rpm) plotted as absorbance versus the square of the radial position as measured from the sample meniscus. The curve fit to the data represents a single exponential fit to the sedimentation equilibrium equation $C_i r = C_i r_m e^{AM_i(r_i^2 - r_m^2)}$ which affords an apparent MW of 1600 (monomer) at 23 °C (0.11 mM, pH 6.8). A partial specific volume for the peptide of 0.84 cm^3/g and a solvent density of 0.998 g/cm^3 were used.

shown by analytical equilibrium ultracentrifugation. The observed molecular weight of 1600 ± 80 (0.11 mM, pH 6.8) compares well to the expected weight (1644) of the monomeric species (Figure 8).

The existence of extended structure within peptide **G** was also supported by FT-IR data. The amide I band which corresponds primarily to the C═O stretching vibration of the peptide bond is very sensitive to the peptide backbone conformation.[23] An absorption between 1620 and 1640 cm^{-1} is indicative of β-sheet structure. An additional weak band at 1670−1695 cm^{-1} is specific to antiparallel β-sheet structure. Unordered peptides generally exhibit a carbonyl stretch at 1644 cm^{-1} and may exhibit an absorption between 1657 and 1663 cm^{-1}.[23j] The FT-IR spectrum of a film of peptide **G** (formed from a 5.3 mM D_2O solution, pH 6.8) revealed a major band at 1631 cm^{-1} consistent with β-sheet structure. Weak absorptions at 1657 and 1687 cm^{-1} were also observed. The latter absorption is consistent with antiparallel structure, and the absorption at 1657 cm^{-1} indicates random structure consistent with structural fraying at the termini. The FT-IR spectrum of the D_2O solution of peptide **G** exhibited absorptions at 1635 and 1684 cm^{-1}, again consistent with β-sheet structure. Absorptions at 1647, 1653, and 1662 cm^{-1} which may arise from unstructured regions of the peptide were also observed. These data suggest a fluctuating β-sheet structure, consistent with the CD data.

Classical NOESY and TOCSY experiments were utilized to make sequence specific resonance assignments for peptide **G**. NOEs between the aromatic protons of residue **1** and the flanking Leu-6 α- and β-protons and the Val-8 γ- and γ'-methyl groups of peptide **G** were observed (Figure 9). NOEs were also evident between the aromatic protons of **1** and the protons of the ethylene spacer between **1** and Val-8. As was seen in peptides **A** and **D**, the observed NOEs for peptide **G** support the existence of a hydrophobic cluster composed of the aromatic skeleton of residue **1** and the hydrophobic residues flanking **1**. Strong interstrand NOEs of the type expected for a β-sheet in a protein are not observed in peptide **G** by 2D NOESY spectroscopy. Difference NOE methods which are currently in progress may reveal weak NOEs. Further evidence that peptide **G** is structured near the biphenyl template was provided by the observed $^3J_{\alpha NH}$ coupling constants of ≥7.5 Hz for the six residues nearest to **1**. Coupling constants in the range of 7.5−10 Hz are expected for a β-sheet or an extended structure.[24]

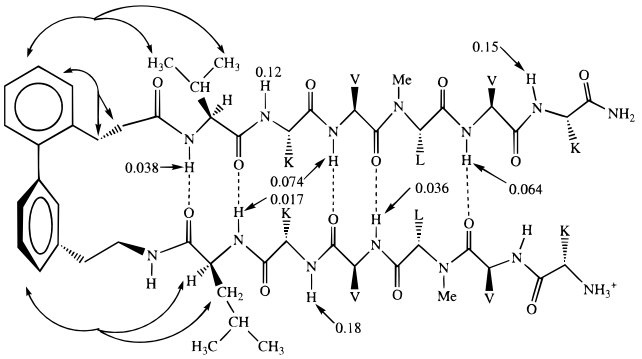

Figure 9. Proposed structure of peptide **G** which is ordered in the vicinity of **1** and less structured at the termini of the strands. Amide proton exchange rates for peptide **G** were obtained from samples which were 2.8−2.9 mM at pH 3.2. The rates (min^{-1}) were determined at 25 °C and averaged over a minimum of three experiments. The NOE data were obtained on a 2.1 mM sample at pH 3.5.

Amide exchange studies at pH 3.2 were used to examine the hydrogen-bonding properties of peptide **G** which is expected to be partially folded on the basis of the studies discussed above. The rates of amide proton exchange for Leu-6 and Val-8 (the residues flanking **1**) as well as Val-4 and Val-10 (the next pair of intramolecular hydrogen-bonded residues in the β-sheet structure) were significantly slower than the measurable rates for the remaining residues (Figure 9). As would be expected for a β-sheet conformation, the solvent-exposed lysine amide NHs exhibited the fastest amide exchange rates. The amide proton/deuterium exchange rates were studied in the random coil peptide **H** (having Gly-Gly in place of **1**, Table 1) to demonstrate that the faster Lys amide exchange relative to the Val exchange was not simply a result of the nature of the side chain. The range of amide exchange rates was very narrow in peptide **H** compared to that of peptide **G**, suggesting that all of the amide protons in peptide **H** are in a nearly equivalent environment as would be expected for an unordered structure. Interestingly, both the slowest and fastest observed rates were for protons corresponding to valine residues in the unordered peptides while the lysine residues generally exhibited intermediate exchange rates. These data support the interpretation that the rate differences observed in peptide **G** are a result of differences in the amide proton environments rather than inherent differences between the valine and lysine amino acids.

The CD and FT-IR data in conjunction with the NMR data support a well-defined structure in the vicinity of **1** with fraying of the β-sheet-like structure near the N- and C-termini. These results confirm that biphenyl-based residue **1** promotes intramo-

(23) (a) Haris, P. I.; Chapman, D. *Biopolymers* **1995**, *37*, 251−263. (b) Byler, D. M.; Susi, H. *Biopolymers* **1986**, *25*, 469−487. (c) Byler, D. M.; van Gusteren, W. F. *FEBS Lett.* **1993**, *323*, 215−217. (d) Surewicz, W. K.; Mantsch, H. H. *Biochim. Biophys. Acta* **1988**, *952*, 115−130. (e) Surewicz, W. K.; Mantsch, H. H.; Chapman, D. *Biochemistry* **1993**, *32*, 389−394. (f) Dong, A.; Caughey, W. S. *Biochemistry* **1990**, *29*, 3303−3308. (g) Krimm, S.; Bandekar, J. *Adv. Protein Chem.* **1986**, *38*, 181−364. (h) Takeda, N.; Kato, M.; Taniguchi, Y. *Biochemistry* **1995**, *34*, 5980−5987. (i) Arrondo, J. L. J.; Young, N. M.; Mantsch, H. H. *Biochim. Biophys. Acta* **1988**, *952*, 261−268. (j) Oberg, K.; Chrunyk, B. A.; Wetzel, R.; Fink, A. L. *Biochemistry* **1994**, *33*, 2628−2634.

(24) Pardi, A.; Billeter, M.; Wüthrich, K. *J. Mol. Biol.* **1984**, *180*, 741−751.

lecular folding to afford a monomeric β-hairpin-like structure. In peptides which are capable of lateral association (such as peptide **D**), the monomeric β-sheets then undergo rapid self-association to form a β-sheet fibril.

Discussion

It is currently possible to induce both α-helical and β-sheet conformations in small peptides by the strategic incorporation of templates into the α-amino acid sequence.[4c] Biphenyl-based amino acid **1** can now be added to the short list of templates useful for nucleating β-sheet structure.

FT-IR and variable temperature NMR studies on diamide derivatives of **1** and **2** have shown that both residues **1** and **2** are capable of promoting hydrogen-bonded conformations which should facilitate β-sheet structure formation in CH_2Cl_2.[7] Amide H−D exchange data suggest that residue **1** can promote a 15-membered ring hydrogen bond between the flanking α-amino acid residues in heptapeptides and tridecameric peptides in aqueous solution. Nuclear overhauser enhancement data on peptides incorporating residues **1** and **2** demonstrate that only residue **1** is capable of promoting a hydrophobic cluster conformation in aqueous solution when flanked in sequence by hydrophobic α-amino acid residues. The hydrogen-bonded hydrophobic cluster conformation is formed even under conditions where β-sheet structure is not observed by far-UV CD (e.g., peptide **D** at low pH). The hydrogen-bonded hydrophobic cluster is apparently poised to nucleate β-sheet folding once solution conditions permit as is seen in peptide **D** where β-sheet folding occurs after the charge density in the strands is reduced by an increase in pH. The importance of the hydrophobic cluster is best illustrated by peptide **F** which can accomplish intramolecular hydrogen bonding but cannot fold under conditions suitable for folding of peptide **D**. The inability of peptide **F** to adopt a folded structure can be explained by the absence of a hydrophobic cluster, owing to the hydrophilic lysine residues flanking **1**. Modeling suggests that one phenyl ring in **1** and one flanking α-amino acid side chain are interacting at a time to form the hydrophobic cluster, in contrast to the planar dibenzofuran-based template which is capable of interacting simultaneously with both of the flanking hydrophobic α-amino acid side chains.[1m] Hence, the stabilization resulting from the hydrophobic cluster appears to be attenuated in the case of **1** relative to that of the dibenzofuran-based template as is evident from the lack of structure in heptapeptides containing **1** and the higher pH required to induce the coil to sheet transition in tridecapeptides containing **1**. However, caution must be exercised when potential nucleators are compared on the basis of pH dependent coil to sheet transitions. A comparison of peptides having identical α-amino acid sequences, but differing in the nucleating residue incorporated (**1** or **2**), strongly suggests that residue **2** is incapable of promoting intramolecular folding, most likely as a consequence of its inability to promote hydrophobic cluster formation.

Since peptide **D** forms a high molecular weight β-sheet fibril, it was necessary to demonstrate that intramolecular folding precedes self-assembly to be confident that **1** was functioning as a folding nucleator. The strategic replacement of two Lys residues in peptide **D** with *N*-methyl-Leu residues proved to be a useful strategy to prevent unwanted β-sheet-mediated self-assembly subsequent to β-hairpin formation. The di-N-methylated sequence (peptide **G**) adopts a monomeric β-sheet-like structure in aqueous solution as discerned by analytical equilibrium ultracentrifugation, far-UV CD, FT-IR, and NMR evidence, substantiating the claim that residue **1** is capable of nucleating an intramolecular β-hairpin structure. Interestingly, the β-hairpin structure in peptide **G** becomes more highly structured with increased temperature as a likely consequence of the temperature dependence of the hydrophobic effect.[9a] Long-range hydrophobic interactions between side chains in the β-sheet portion and the localized hydrophobic interactions in the cluster promoted by **1** likely contribute to the temperature dependent increase in β-hairpin stability in peptide **G**. A temperature dependent increase in structure is rare, but has been observed previously by Urry and seems to be general for the related β-hairpin structures we have examined which are stabilized by hydrophobic interactions.[22,25] The fact that the β-hairpins templated by **1** become more structured at 37 °C could prove to be very important in medicinal chemistry applications.

Conclusion

Residue **1** promotes a hydrogen-bonded, hydrophobic cluster conformation in aqueous solution which induces intramolecular β-hairpin folding. Subsequent self-assembly of the β-hairpin is normally observed, but can be prevented by the strategic incorporation of N-methylated amino acids into peptides containing residue **1**. Importantly, residue **1** is effective in nucleating a well-defined, pH independent, monomeric β-sheet-like structure in peptide **G** in aqueous solution, extending the availability of known compounds that function as sheet nucleators. To the best of our knowledge, peptide **G** represents the first example of a peptidomimetic that adopts a monomeric β-hairpin-like structure in aqueous buffers.

Experimental Section

General Methods. Unless otherwise noted, materials were obtained from commercial suppliers and were used without further purification. Analytical thin layer chromatography was performed on E. Merck silica gel 60 F_{254} plates. Column chromatography was performed as described by Still[26] using forced flow (flash) chromatography with the indicated solvents on Baxter SIP silica gel, 60 Å (230−400 mesh). High-resolution mass spectra were obtained on a VG-70S double-focusing high-resolution mass spectrometer. Ultraviolet spectra were obtained on a Milton Roy Spectronic 3000 diode array spectrophotometer. Analytical and preparative HPLC was carried out on a dual pump system equipped with Altex 110A pumps and a 420-gradient programmer or a Waters 600 preparative HPLC. Waters RCM Delta Pak C_{18} and C_4 (15 μm, 300 Å, 25 × 100 mm) columns and a Knauer 86 variable-wavelength detector were used. Solvent A was composed of 95% water, 5% acetonitrile, and 0.2% TFA. Solvent B was composed of 5% water, 95% acetonitrile, and 0.2% TFA.

Preparation of Boc-Leu-2-CO_2H (3) for Incorporation into Peptide E. Methyl 2-amino-3′-biphenylcarboxylate[7] (176.7 mg, 0.78 mmol) was dissolved in CH_2Cl_2/DMF (20 mL of a 9:1 mixture) in a 50 mL round-bottomed flask. To the dark yellow solution were added Boc-Leu·H_2O (1.94 g, 7.78 mmol), DIEA (1.70 mL, 9.76 mmol), and BOP reagent (3.51 g, 7.94 mmol). The reaction mixture was stirred at room temperature under N_2 for 42 h. *N,N′*-Dimethylethylenediamine (1.7 mL, 16 mmol) was added, and the mixture was stirred for 2 h to destroy the excess HOBt active ester. The reaction mixture was transferred to a separatory funnel and washed with 1 M citric acid (3 × 25 mL), 5% $NaHCO_3$ (2 × 35 mL), and H_2O (50 mL). The organic layer was dried ($MgSO_4$), concentrated in vacuo, and further dried under high vacuum to afford a beige solid. The crude material was dissolved in anhydrous MeOH (50 mL), and NaOH was added (13.0 mL of a 0.59 M solution in MeOH, 7.7 mmol). The clear yellow solution was heated at reflux for 72 h. The reaction mixture was concentrated, and the yellow residue was partitioned between CH_2Cl_2 and H_2O (100 mL each). The aqueous layer was washed with CH_2Cl_2 (3 × 100 mL). The combined organic layers were washed with H_2O (100 mL), dried

(25) Choo, D. W.; Fiori, W. R.; Kelly, J. W. Unpublished results.
(26) Still, W. C.; Kahn, M.; Maitra, A. *J. Org. Chem.* **1978**, *43*, 2923−2925.

($MgSO_4$), concentrated in vacuo, and further dried under high vacuum to afford 1.37 g of a light yellow residue. The material was purified by flash chromatography (70:30 to 50:50 hexanes/ethyl acetate) to afford 0.302 g (89%) of a white solid: MALDI-TOFMS (MH^+) *m/z* calcd 427.2, obsd 427.7; MS (+FAB, NBA/PEGH) *m/z* 427.2237, $[M + H]^+$ calcd for $C_{24}H_{30}O_5N_2$, 427.2233.

Synthesis of Peptides A−G. Manual solid phase peptide synthesis was carried out using the benzhydrylamine resin available from Advanced Chemtech. The resins used had a loading of 0.70 or 0.55 mequiv/g. Reagent grade dichloromethane, isopropyl alcohol (IPA), and *N*,*N*-dimethylformamide (DMF) were used. DMF was stored over 4 Å molecular sieves. Side chain protected Boc-amino acids were purchased from Advanced Chemtech. Trifluoroacetic acid (TFA) was purchased from Solvay Performance Chemicals and was used as a 35% solution in CH_2Cl_2 containing 1% thioanisole as a scavenger. *N*,*N*-Diisopropylethylamine (DIEA) was refluxed over ninhydrin, distilled, and then distilled from calcium hydride. The first amino acid was loaded onto the resin by shaking 1.6 equiv of the diisopropylcarbodiimide-activated amino acid with the resin for 24 h. The resin was washed with DMF (2 × 1 min), IPA (1 × 1 min), CH_2Cl_2 (1 × 1 min), IPA (1 × 1 min), CH_2Cl_2 (1 × 1 min), IPA (1 × 1 min), and CH_2Cl_2 (4 × 1 min). The Kaiser ninhydrin test was used to monitor completion of all couplings. If the test was slightly positive, the unreacted amino groups were acetylated with acetic anhydride or the peptide was recoupled. Standard couplings were performed in the following manner: TFA prewash (35% TFA × 1 min), TFA deprotection (35% TFA × 50 min), CH_2Cl_2 (2 × 1 min), IPA (1 × 1 min), CH_2Cl_2 (1 × 1 min), IPA (1 × 1 min), CH_2Cl_2 (4 × 1 min), preneutralization (12% DIEA × 1 min), neutralization (12% DIEA × 9 min), CH_2Cl_2 (4 × 1 min), coupling (3 equiv of amino acid, 3 equiv of BOP, 4 equiv of DIEA in CH_2Cl_2 containing 10−15% DMF for 2−8 h), DMF (2 × 1 min), IPA (1 × 1 min), CH_2Cl_2 (1 × 1 min), IPA (1 × 1 min), CH_2Cl_2 (1 × 1 min), IPA (1 × 1 min), CH_2Cl_2 (4 × 1 min). The dipeptide Boc-Leu-**2**-CO_2H (**3**) was incorporated into peptide **E** by shaking the preneutralized resin with 1.8 equiv of **3**, 2 equiv of BOP, and 3.2 equiv of DIEA in CH_2Cl_2 containing 10−15% DMF for 15 h. The Boc-protected analogue of amino acid **1** (3′-[2-[*N*-(*tert*-butyloxycarbonyl)amino]ethyl]-2-biphenylpropionic acid, compound **4**)[7] was incorporated into peptides **A**−**D**, **F**, and **G** by shaking 0.6−3.0 equiv of preneutralized resin with 1.0 equiv of **4**, 1.1 equiv of BOP, and 1.4 equiv of DIEA in CH_2Cl_2 containing 10−15% DMF for 40−66 h. Peptide **G** was subjected to three valine couplings (6 equiv of valine, 6 equiv of BOP, 8 equiv of DIEA) after incorporation of each of the *N*-methylleucine residues. The resin was then capped with acetic anhydride, and subsequent couplings were performed as described above. Upon completion, the resin-bound peptides were treated with TFA to remove the Boc group, dried under high vacuum, and treated with HF[16] to deprotect the side chains and cleave the peptide from the resin. The crude peptides were purified by preparative C_{18} HPLC. All peptides were characterized by matrix-assisted laser desorption ionization time-of-flight mass spectrometry (MALDI-TOFMS).[17a]

Summary of Purification and Characterization of Peptides A−G. Peptide A ($C_{49}H_{80}N_{10}O_7$). ^+H_3N-VOL-**1**-VOL-C(O)NH_2. Purification by preparative C_{18} HPLC employing a linear gradient from 20% to 60% solvent B over 20 min: overall yield 47%; MALDI-TOFMS $[M + H]^+$ *m/z* obsd 922.3, calcd 922.3.

Peptide B ($C_{52}H_{78}N_{10}O_7$). ^+H_3N-VOF-**1**-VOL-C(O)NH_2. Purification by preparative C_{18} HPLC employing a linear gradient from 30% to 60% solvent B over 20 min: overall yield 32%; MALDI-TOFMS $[M + H]^+$ *m/z* obsd 956.4, calcd 956.3.

Peptide C ($C_{80}H_{77}N_9O_9$). ^+H_3N-VEL-**1**-VOL-C(O)NH_2. Purification by preparative C_{18} HPLC employing a linear gradient from 30% to 60% solvent B over 20 min: overall yield 41%; MALDI-TOFMS $[M + H]^+$ *m/z* obsd 937.5, calcd 937.2.

Peptide D ($C_{84}H_{148}N_{20}O_{13}$). ^+H_3N-$(KV)_2$KL-**1**-$(VK)_3$-C(O)NH_2. Purification by preparative C_{18} HPLC employing a linear gradient from 10% to 60% solvent B over 20 min: overall yield 64%; MALDI-TOFMS $[M + H]^+$ *m/z* obsd 1647.3, calcd 1647.3.

Peptide E ($C_{80}H_{140}N_{20}O_{13}$). ^+H_3N-$(KV)_2$KL-**2**-$(VK)_3$-C(O)NH_2. Purification by preparative C_{18} HPLC employing a linear gradient from 10% to 40% solvent B over 20 min: overall yield 17%; MALDI-TOFMS $[M + H]^+$ *m/z* obsd 1591.1, calcd 1591.1.

Peptide F ($C_{83}H_{146}N_{20}O_{13}$). ^+H_3N-$(VK)_3$-**1**-$(KV)_3$-C(O)NH_2. Purification by preparative C_{18} HPLC employing a linear gradient from 20% to 60% solvent B over 20 min: overall yield 23%; MALDI-TOFMS $[M + H]^+$ *m/z* obsd 1632.9, calcd 1633.2.

Peptide G ($C_{86}H_{150}N_{18}O_{13}$). ^+H_3N-KV-(NMe)L-VKL-**1**-VKV-(NMe)L-VK-C(O)NH_2. Purification by preparative C_{18} HPLC employing a linear gradient from 20% to 60% solvent B over 25 min: MALDI-TOFMS $[M + H]^+$ *m/z* obsd 1644.8, calcd 1645.2.

Circular Dichroism Studies of Peptides A−G. CD spectra were obtained on a Jasco J-600, an Aviv 62DS, or an Aviv 62ADS spectropolarimeter. The data were imported into the Macintosh version of KaleidaGraph and processed. The samples were prepared as stock solutions in water and diluted to the desired concentration in 10 mM buffer. The concentrations of peptides **A**−**G** were calculated on the basis of mass. The samples were allowed to equilibrate at 25 °C for 18−24 h prior to the CD experiments. Data were collected at 25 °C using a scan speed of 20 nm/min (Jasco spectropolarimeter), a time constant of 0.5 s, and a band width of 1 nm. Spectra were corrected for buffer contributions and are reported in mean residue ellipticity.[27]

^{1}H NMR Studies of Peptides A and D−G. All ^{1}H NMR studies of peptides **A** and **D**−**G** were performed on a Varian UnityPlus 500 NMR spectrometer. Data from the 500 MHz NMR were processed using Varian VNMR version 5.1 software. Samples used for 1-D, 2-D, and variable temperature studies were prepared in 10 mM borate buffer, 90:10 H_2O/D_2O, and contained 0.02% sodium azide. All samples were referenced to DSS (0 ppm). In the cases of peptides **A** and **D**, the TOCSY and ROESY experiments were obtained at 25 and 5 °C as it was possible to observe several amide protons at 5 °C which were not observed at 25 °C due to exchange with the D_2O. TOCSY spectra of peptides **E**−**G** were obtained at 25 °C. ROESY experiments were obtained with a mixing time of 300 ms for peptide **A** and 150 ms for peptides **D**−**G**.

Proton 1- and 2-D experiments were obtained for peptide **A** on a 2.4 mM sample at pH 7.3, for peptide **D** on a 5.0 mM sample at pH 6.3, for peptide **E** on a 2.4 mM sample at pH 7.0, for peptide **F** on a 2.1 mM sample at pH 7.9, for peptide **G** on a 2.9 mM sample at pH 3.5 (10 mM acetate buffer, 90:10 H_2O/D_2O), and for peptide **H** on a 1.9 mM sample at pH 3.5.

Amide exchange experiments for peptides **A**, **D**, and **G** were repeated 3−4 times, and the averaged results were reported. Peptide **D** was 2.5−2.9 mM, pH 4.1−5.1. Peptide **A** was 3.0−3.3 mM, pH 3.4−3.6. Peptide **G** was 2.8−2.9 mM, pH 3.2. Peptide **H** was 1.9 mM, pH 4.0. The studies were done by dissolving the peptide in D_2O and obtaining the first spectrum as quickly as possible. Generally, the time from mixing to completion of data collection for the first spectrum was 5 min (time 0). Subsequent spectra were obtained every 3.4 min for the first 60 min and then every 6.3 min for the next 60 min. The amide peak heights were normalized using the aromatic triplet at 7.45 ppm as a standard for each spectrum. The exchange rates were then obtained from a plot of $\ln(H_o/H_t)$ versus time, where H_o is the amide peak height at time 0 and H_t is the amide peak height at time *t*.

It should be noted that NMR samples of peptides **A** and **D**−**F** were prepared at pH values which are well below those at which β-sheet structure is observed by CD. This was due to the fact that, at concentrations relevant for the NMR studies, peptides samples which were prepared at higher pH values gelled and were thus unsuitable for the NMR studies.

Electron Microscopy of Peptide D. Electron micrographs of peptide **D** were obtained from samples prepared with 10 mM borate buffer at pH 10.2. The peptide sample was incubated for 24 h at 25 °C. Samples were applied to a carbon-coated copper grid for 1−2 min. Excess solution was removed by blotting with filter paper. The sample was then stained with Ruthenium Red stain (1.5% in 0.1 M ammonium hydroxide) for 10 min, and the excess staining solution was removed. The fibrils were examined on a Zeiss 10C electron microscope operating at 60 kV. Concentrations of 20, 100, and 200

(27) *Protein Structure: A Practical Approach*; Creighton, T. E., Ed.; IRL Press: Oxford, 1989; pp 251−285.

(28) This figure was prepared with MolScript; see: Kraulis, P. T. *J. Appl. Crystallogr.* **1991**, *24*, 946−950.

μg/mL afforded fibrils which were typically of dimensions ~30 Å by 500−1000 Å. Associated fibrils had widths which were greater than 50 Å.

Sedimentation Equilibrium Analytical Ultracentrifugation Studies of Peptides D and G. The apparent molecular weights of peptides **D** and **G** were obtained from data collected on a Beckman XL-A analytical ultracentrifuge equipped with absorption optics. A double-sector cell equipped with a 12 mm Epon centerpiece and sapphire windows was used. Samples were loaded into the cell using a blunt end microsyringe, resulting in a column height of approximately 3 mm. The samples were prepared from stock solutions in water and diluted to the appropriate concentration in 10 mM borate buffer. Peptide **D** was 0.15 mM at pH 9.1, and samples of peptide **G** were 0.11 mM at pH 6.8, 0.25 mM at pH 7.3, and 0.41 mM at pH 6.9. In a typical experiment, an initial absorbance scan was performed at 23 °C with a rotor speed of 3000 rpm. The rotor speed was then increased to 60 000 rpm where sedimentation was established. A complete loss of the initial absorbance is indicative of a highly associated system.

FT-IR Studies of Peptide G. A 5.3 mM D_2O solution (pH 6.8) of the chloride salt of peptide **G** was prepared and incubated at 25 °C for 12 h. The IR spectra were collected on a Galaxy 6021 spectrometer equipped with an MCT detetctor. The film was cast on a ZnSe plate, and the D_2O solution spectrum was obtained using a CaF_2 solution cell with an optical path length of 0.02 mm. In both cases, 2048 scans were obtained for the sample and background.

Acknowledgment. We thank Professor Timothy Hayes for allowing us to perform HF cleavages in his laboratory, Professor David Russell for providing access to and assistance with MALDI-TOFMS, and Professor Donald Darensbourg for providing access to FT-IR facilities. We also thank Joel Schneider and Hilal Laushel for carrying out the ultracentrifuge studies, Steve Silber, Wayne Fiori, Nilsa Graciani, and Robert Espina for obtaining the peptide NMR data, and Danny Choo for the synthesis and purification of peptide **H**. We gratefully acknowledge financial support from the National Institutes of Health (Grant R01 GM51105), the Robert A. Welch Foundation, Searle Scholars Program/The Chicago Community Trust (J.W.K.), and the Camille and Henry Dreyfus Foundation Teacher Scholars Program (J.W.K.), the National Science Foundation (Grant 9217413) for providing the 500 MHz NMR, and the Center for Macromolecular Design for support of the biophysical instrumentation.

JA952472X